Shell-model study of $^{39}S(\beta^-)^{39}Cl$ and the energy levels of ^{39}Cl

E. K. Warburton
Brookhaven National Laboratory, Upton, New York 11973
and Physikalisches Institut der Universität Heidelberg and Max-Planck-Institut für Kernphysik, D-6900 Heidelberg, Federal Republic of Germany

J. A. Becker
Lawrence Livermore National Laboratory, Livermore, California 94550
(Received 14 August 1989)

Shell-model calculations are performed for the odd- and even-parity states of ^{39}Cl and the odd-parity states of ^{39}S. The ^{39}S odd-parity states and the ^{39}Cl even-parity states were considered in full $(1s,0d)^{20}(0f,1p)^3$ and $(1s,0d)^{21}(0f,1p)^2$ configurational spaces, respectively. For the ^{39}Cl odd-parity states it was necessary to use a highly truncated $(1s,0d)^{20}(0f,1p)^3$ configurational space. The method and results of truncation are discussed in some detail. Observables calculated include energy spectra, binding energies, $^{40}Ar \rightarrow {}^{39}Cl + p$ spectroscopic factors, first-forbidden and allowed β^- decay of ^{39}S, and γ transitions in both ^{39}S and ^{39}Cl. Results are compared to experiment. For example, the spectroscopic factors for $1/2^+$ and $3/2^+$ ^{39}Cl states and the γ transitions between the even-parity ^{39}Cl states are predicted with high accuracy while the half-life of ^{39}S is calculated to be 5.6 s (if the spin-parity of ^{39}S has the preferred value of $7/2^-$) as compared to the experimental value of 11.5 ± 0.5 s.

I. INTRODUCTION

We present here shell-model predictions for the β^- decay of ^{39}S and the spectroscopy of ^{39}S and ^{39}Cl. The shell-model calculations are similar to those made previously for ^{40}S and ^{40}Cl (Ref. 1). The Warburton, Becker, Millener, and Brown (WBMB) interaction used in these studies is designed to describe nuclear levels in the $A=31$–44 region for which the nucleons occupy the seven subshells of the (sd) and (fp) major shells. Hamiltonian diagonalization is carried out in the $(2s,1d)^{A-16-n}(1f,2p)^n$ model space for a single value of n. We shall refer to this as the nfp model space.

There have been no previously reported shell-model calculations for ^{39}S or the $3fp$ states of ^{39}Cl. Calculations for the $2fp$ states of ^{39}Cl were performed with an interaction very similar to this one for the purpose of calculating the beta decay of ^{39}Cl (Ref. 2) and the energy spectrum from this calculation was included in an informal report on the WBMB interaction.[3] A ^{39}Cl $2fp$ energy spectrum was also reported by Woods[4] who used a model space of $(d_{3/2},s_{1/2})^9(f_{7/2},p_{3/2})^3$; i.e., the $sdfp$ space was truncated by omitting the $d_{5/2}$, $f_{5/2}$, and $p_{1/2}$ orbits. As discussed in Sec. III, our calculations indicate that this truncation is not too drastic for the calculation of the ^{39}Cl even-parity energy spectrum which was all that Woods considered.

The beta decay of ^{39}S, which is the main subject of this paper, was first observed and studied by Hill, Petry, and Wang.[5] There have been no subsequent reports on this decay. The half-life was measured to be 11.5(5) s and γ transitions involving five excited states of ^{39}Cl were observed. Since ^{39}S has $N=23$, the $3fp$ model space is appropriate for its wave functions. ^{39}S will decay by allowed β^- transitions to $3fp$ states of ^{39}Cl and by first-forbidden β^- transitions to $2fp$ states. We will consider both of these types of decay.

^{39}Cl itself decays by β^- emission to ^{39}Ar (Refs. 2 and 6) and the decay modes establish the ^{39}Cl ground state as $3/2^+$. In addition to beta decay, information on the energy levels of ^{39}Cl has been deduced from the $^{40}Ar(d,{}^3He)^{39}Cl$ (Refs. 7 and 8) and $^{37}Cl(t,p\gamma)^{39}Cl$ (Ref. 9) reactions. We shall consider aspects of both studies.

II. THE CALCULATION

A. The interaction

The WBMB interaction for the $sdfp$ model space is derived from an effective one-body plus two-body Hamiltonian and is composed of three parts. The starting point is the "universal" $(1s,0d)$ interaction, denoted USD, of Wildenthal.[10] Interactions between $(0f,1p)$ nucleons are accounted for by an interaction developed by McGrory[11] and the cross-shell interaction connecting the $(1s,0d)$ and $(0f,1p)$ shells was generated from the nucleon-nucleon potential of the Millener-Kurath interaction.[12] The relative single-particle energies of the three sd shell orbits and the four fp shell orbits were taken from the USD and McGrory interactions, respectively. The energy gap between the sd and fp shells was determined from a consideration of binding energies of $A=35$–43 nuclei.[3] The calculation is performed with OXBASH (Ref. 13) using both isospin and proton-neutron formalisms. Details of calculations using OXBASH with the WBMB interaction have been given previously.[1,3]

B. The model space and its truncation for the $3fp$ ^{39}Cl states

The J matrices of the $2fp$ states of ^{39}Cl have a dimension, $D(J)$, which has its maximum of 858 for $J^\pi=7/2^+$; while for the $3fp$ states of ^{39}S $D(J)$ is 9045 for $J^\pi=7/2^-$. Until recently, our disc-space resources allowed us to diagonalize J matrices up to a dimension, $D(J)$, of about 6000 depending on the m dimension, $D(m)$. A recent increase in disc storage capacity allowed us to diagonalize the complete $3fp$ spectrum of ^{39}S. The $3fp$ model space of ^{39}Cl has a $D(J)$ of 25 031 ($\sim$65 200) for $J^\pi=1/2^-(7/2^-)$. It is necessary to truncate severely.

In OXBASH, truncation can be accomplished by selection of partitions; a partition being a specific occupancy of the subshells included in the interaction. We designate a partition $\mathcal{P}$ as

$$\mathcal{P}=[n(d_{5/2}),n(d_{3/2}),n(s_{1/2})|n(f_{7/2}),n(f_{5/2}),n(p_{3/2}),n(p_{1/2})]\ , \tag{1}$$

where $n(j)$ is the occupancy of the subshell j. The method of truncation used for the $3fp$ model space of ^{39}Cl was that designated SPET by Brussaard and Glaudemans.[14] With the single-particle energy associated with the subshell j designated as $\epsilon(j)$, the zeroth-order partition energy for the kth partition was defined as

$$\mathcal{E}(k)=\left[\sum\epsilon(j)\right]_k-\left[\sum\epsilon(j)\right]_{k_0}\ , \tag{2}$$

where the k_0th partition is the one with the lowest value of $\mathcal{E}(k)$ and the sums run over all active nucleons—23 in this case. Each partition also has a J dimension, $D_k(J)$. The partitions were ordered by $\mathcal{E}(k)$ and a cutoff was imposed at the value of k, k_c, for which $\sum_{k=1}^{k_c}D_k(7/2)$ was near the largest possible for the available disk space. This included 75 of the 277 partitions of the full $3fp$ model space and gave $\sum_{k=1}^{75}D_k(7/2)=8949$. For the 75th partition the energy $\mathcal{E}(k)$ is 16.4 MeV.

The main virtue of this truncation scheme is its simplicity. The zeroth-order energy $\mathcal{E}(k)$ represents completely noninteracting particles in an harmonic oscillator basis—a seemingly drastic assumption. The validity of the method depends on $\mathcal{E}(k_c)$ being large compared to the energy spreads due to the effective interactions between nucleons. We can diagonalize individual partitions and groups of partitions in order to illustrate these relative values. We choose $J=1/2$ for these examples because $\sum_{k=1}^{75}D_k(1/2)=3415$ is small enough so that we can also illustrate the effect of significantly increasing the number of partitions. Designating the "ground-state" energy of the diagonalized lth through mth partitions as $\mathcal{E}_B[J;l,m;\sum_{k=1}^{m}D_k(J)]$ we find

$$\mathcal{E}_B[1/2;75,75;41]-\mathcal{E}_B[1/2;1,1;6]=14.5\ \text{MeV}$$

and

$$\mathcal{E}_B[1/2;72,78;152]-\mathcal{E}_B[1/2;1,1;6]=12.0$$

as compared to $\mathcal{E}(75)=16.4$ MeV. Indeed, in this case, the residual interaction appears to be sufficiently small compared to $\mathcal{E}(75)$ for the truncation scheme to be effective. Now consider the composition of the $J=\frac{1}{2}$ wave functions. The first seven of the 75 partitions have $\sum_{k=1}^{7}D_k(1/2)=131$ and for the lowest eigenenergy make up 80.5% of the wave function; while the last seven partitions have $\sum_{k=69}^{75}=629$ and make up 0.17% of the wave function. For the tenth eigenenergy, which lies at 2.8 MeV, these percentages are 61.1% and 0.35%, respectively. The effect of truncation of the $3fp$ space was further explored by increasing k_c from 75 to 84 with $\sum_{k=1}^{84}D_k(1/2)=4298$, and $\mathcal{E}(84)=17.3$ MeV. The percentage of the wave function in partitions $k=76$–84 was found to be 0.86% and the ground-state binding energy for $k_c=84$ was 140 keV more bound that for $k_c=75$.

C. Spuriosity and its elimination

The $2fp$ ^{39}Cl and $3fp$ ^{39}S wavefunctions were generated in the full $sdfp$ model space from configurations which are the lowest allowed by the Pauli principle and thus the wave functions contain no spurious center-of-mass components.[14] The model space for the $2fp$ ^{39}Cl states is

$$(0p)^{12}(1s,0d)^{21}(0f,1p)^2$$

or, more simply,

$$\pi(1s,0d)^{-3}\nu(0f,1p)^2\ . \tag{3}$$

A complete basis for the odd-parity states of ^{39}Cl includes all possible $1\hbar\omega$ excitations of Eq. (3), i.e.,

$$(0p)^{12}(1s,0d)^{20}(0f,1p)^3+(0p)^{11}(1s,0d)^{22}(0f,1p)^2+(0p)^{12}(1s,0d)^{21}(0f,1p)^1(0g,1d,2s)^1\ . \tag{4}$$

We include only contributions from the first term of Eq. (4) in our $3fp$ calculation for ^{39}Cl. Because of the $\Delta\hbar\omega=0$ selection rule on its operator, this omission should not effect the Gamow-Teller matrix elements very much. Certainly the error due to this omission will be small compared to that due to the truncation of the $3fp$ model space just described.

Neglect of the last two terms of Eq. (4) and/or the truncation of the $3fp$ model space for ^{39}Cl will cause some spurious center-of-mass motion. In calculations in OXBASH using the isospin formalism spuriosity is routinely eliminated by the *approximate* method of Gloeckner and Lawson.[15] In this method a Hamiltonian, H_{new}, is constructed which is the sum of the usual shell-model Hamiltonian, H_{SM}, plus the Hamiltonian for the center-of-mass motion, $H_{\text{c.m.}}$, multiplied by a factor larger than

unity, typically ~ 100, e.g.,

$$H_{\text{new}} = H_{\text{SM}} + 100 H_{\text{c.m.}} \ . \tag{5}$$

New shell-model wave functions are now generated with H_{new} in the expectation that only those with large spurious components will significantly increase their eigenenergies. Tests that have been made with this method[3,16] indicate that it is very well suited to cross-shell interactions such as the present WBMB interaction and the similar Millener-Kurath interaction.[12] For instance, use of the Gloeckner-Lawson method with the Millener-Kurath interaction has been examined analytically for several simple cases near $A=16$ where the excitations $0s \rightarrow 0p$ and $(1s0d) \rightarrow (0f,1p)$ were neglected but the full $(0p)(1s,0d)$ space was retained,[16] i.e., the $A \sim 16$ analog of taking only the first term of Eq. (4) for $A \sim 40$. It was found that the spuriosity was removed with negligible error. The effect of spurious center-of-mass motion in this case was explicitly examined by diagonalizing the $J^\pi = \frac{1}{2}^-$ states with the multiplicative factor of Eq. (5) equal to 1 as well as 100. The differences in the eigenenergies and wave functions of the first 50 states considered were very small. We conclude that the effect of spuriosity is negligible compared to the other uncertainties in the calculation such as that due to truncation of the $3fp$ model space.

III. RESULTS

A. Wave functions, spectra, and binding energies

The compositions of the $2fp$ $J^\pi \leq 7/2^+$ yrast states of ^{39}Cl are shown in Table I, and the compositions of the $3fp$ $3/2_1^-$ and $7/2_1^-$ states of ^{39}S and ^{39}Cl are listed in Table II. The predicted spectra are given in Table III. We first consider the $2fp$ ^{39}Cl levels. As expected, the largest component in the yrast $J=3/2$, $5/2$, and $7/2$ states is $(d_{3/2}^{-3})(f_{7/2}^2)$; however, the percentages are small enough so that a simple $(d_{3/2},f_{7/2})^7$ model would appear to be of limited usefulness. It is seen that the wave functions are relatively simple only in the sense that just ten of the allowable 90 partitions comprise $>95\%$ of the wave functions. The contribution of the energy-unfavored $p_{1/2}$, $f_{5/2}$, and $d_{5/2}$ orbits are very similar to those found in our related study of ^{40}Cl (Ref. 1). A truncation eliminating these orbits would appear to be feasible for some studies, but the role in β and γ matrix elements of the $d_{5/2}$ orbit in particular is non-negligible.

The wave functions of the ^{39}S $3/2_1^-$ and $7/2_1^-$ states (Table II) are somewhat more complex than the ^{39}Cl states of Tables I and II. This is expected for several reasons, one of which is that the energy-unfavored proton orbits are more important than for the ^{39}Cl yrast states (compare Tables I and II) since they are closer to the Fermi surface. We find that the wave functions of the ^{39}Cl $3fp$ levels are almost pure neutron excitations of the $2fp$

TABLE I. Composition of the $1/2_1^+$, $3/2_1^+$, $5/2_1^+$, and $7/2_1^+$ ^{39}Cl wave functions. Only those partitions are listed which have contributions of $>1.0\%$ to one of the four states. The three lines at the bottom give the total contribution of the energy-unfavored orbits.

Partition	Configuration	^{39}Cl intensity (in %) $1/2_1^+$	$3/2_1^+$	$5/2_1^+$	$7/2_1^+$
[12,5,4;2,0,0,0]	$(d_{3/2}^{-2})(f_{7/2}^2)$	6.50	70.45	59.18	61.15
[12,6,3;2,0,0,0]	$(d_{3/2}^{-2}s_{1/2}^{-1})(f_{7/2}^2)$	61.41	5.52	17.79	6.93
[12,7,2;2,0,0,0]	$(d_{3/2}^{-1}s_{1/2}^{-2})(f_{7/2}^2)$	0.75	1.79	2.50	1.19
[10,7,4;2,0,0,0]	$(d_{5/2}^{-2}d_{3/2}^{-1})(f_{7/2}^2)$	0.45	2.70	2.30	2.30
[11,6,4;2,0,0,0]	$(d_{5/2}^{-1}d_{3/2}^{-2})(f_{7/2}^2)$	1.67	2.55	1.80	1.48
[11,7,3;2,0,0,0]	$(d_{5/2}^{-1}d_{3/2}^{-1}s_{1/2}^{-1})(f_{7/2}^2)$	3.00	1.08	1.69	1.18
[10,8,3;2,0,0,0]	$(d_{5/2}^{-2}s_{1/2}^{-1})(f_{7/2}^2)$	1.35	0.05	0.18	0.09
[12,5,4;1,0,1,0]	$(d_{3/2}^{-3})(f_{7/2}^1p_{3/2}^1)$	12.24	1.52	5.70	15.28
[12,6,3;1,0,1,0]	$(d_{3/2}^{-2}s_{1/2}^{-1})(f_{7/2}^1p_{3/2}^1)$	2.64	2.21	2.87	2.56
[12,6,3;0,0,2,0]	$(d_{3/2}^{-2}s_{1/2}^{-1})(p_{3/2}^2)$	3.42	0.16	0.91	0.08
[12,5,4;0,0,2,0]	$(d_{3/2}^{-3})(p_{3/2}^2)$	0.52	5.37	0.66	2.12
[12,5,4;0,0,1,1]	$(d_{3/2}^{-3})(p_{3/2}^1p_{1/2}^1)$	0.25	0.17	0.35	1.08
[12,6,3;0,2,0,0]	$(d_{3/2}^{-2}s_{1/2}^{-1})(f_{5/2}^2)$	2.41	0.12	0.52	0.02
[12,5,4;0,2,0,0]	$(d_{3/2}^{-3})(f_{5/2}^2)$	0.08	3.14	0.24	0.32
Sum		96.69	96.83	96.69	95.78
$p_{1/2}$ orbit		1.64	1.82	1.60	2.55
$f_{5/2}$ orbit		3.63	4.20	1.94	5.53
$n(d_{5/2})<12$		8.09	7.57	8.86	6.73

states. Thus the allowed β^- decay proceeds via nearly pure $\nu(sd) \rightarrow \pi(sd)$ transitions and these are largely $\nu d_{3/2} \rightarrow \pi d_{3/2}$ with small interference contributions from the other possible single-nucleon transitions.

The energy levels and binding energy of ^{39}S have been studied by Drumm *et al.*[17] using the ^{40}Ar(^{13}C, ^{14}O)^{39}S reaction. They report a binding energy of 325 430(50) keV and the observation of an excited state of 1469(25) keV. However, as seen in Table III, our prediction is for the 3/2, 5/2, and 7/2 yrast states of ^{39}S to lie uncomfortably close together compared to the energy resolution of the experiment.[18] Thus it is not clear whether the experimental binding energy represents a composite of two or three levels or, if only one level is dominant, that it is the ground state. Nevertheless, for simplicity, we shall assume that the measured binding energy is that of the ground state. The experimental binding energy of ^{39}Cl is 331 287(19) keV (Ref. 19). Thus the ^{39}S(β^-)^{39}Cl Q_β value is 6640(53) keV. The WBMB interaction has good predictive powers for binding energies. For 14 $N=21$ and 22 nuclei in the $A=35$–42 region, the mean deviation from experimental binding energies is 236 keV (Ref.

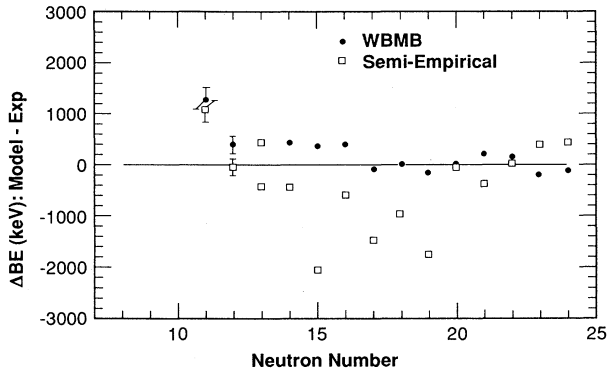

FIG. 1. Comparison of experimental and predicted binding energies for the sulfur isotopes. Binding energies are taken to be positive. The abscissa gives the difference between the predictions and experiment. For $N \leq 20$ the shell-model predictions are from the USD (Ref. 10) and replicated by the WBMB, for $N > 20$ they are from the WBMB. The predictions of the semi-empirical mass formulae are those of Möller, *et al.* (Ref. 20).

TABLE II. Composition of the $3/2_1^-$, and $7/2_1^-$ ^{39}S and ^{39}Cl wave functions. Only those partitions are listed which have contributions of $>0.6\%$ to one of the four states. The three lines at the bottom give the total contribution of the energy-unfavored orbits.

		Intensity (in %)			
		^{39}S		^{39}Cl	
Partition	Configuration	$3/2_1^-$	$7/2_1^-$	$3/2_1^-$	$7/2_1^-$
[12,4,4;3,0,0,0]	$(d_{3/2}^{-4})(f_{7/2}^{3})$	16.44	41.14	48.82	56.77
[12,6,2;3,0,0,0]	$(d_{3/2}^{-2}s_{1/2}^{-2})(f_{7/2}^{3})$	10.03	14.59	3.68	4.85
[12,5,3;3,0,0,0]	$(d_{3/2}^{-3}s_{1/2}^{-1})(f_{7/2}^{3})$	13.46	7.50	17.25	7.98
[10,6,4;3,0,0,0]	$(d_{5/2}^{-2}d_{3/2}^{-2})(f_{7/2}^{3})$	1.89	6.95	3.14	3.27
[11,5,4;3,0,0,0]	$(d_{5/2}^{-1}d_{3/2}^{-3})(f_{7/2}^{3})$	0.37	5.23	3.36	3.72
[11,6,3;3,0,0,0]	$(d_{5/2}^{-1}d_{3/2}^{-2}s_{1/2}^{-1})(f_{7/2}^{3})$	1.29	4.48	2.49	1.30
[12,5,3;2,0,1,0]	$(d_{3/2}^{-3}s_{1/2}^{-1})(f_{7/2}^{2}p_{3/2}^{1})$	6.39	1.98	3.90	3.79
[12,6,2;2,0,1,0]	$(d_{3/2}^{-2}s_{1/2}^{-2})(f_{7/2}^{2}p_{3/2}^{1})$	7.22	1.94	1.03	0.59
[12,4,4;2,0,1,0]	$(d_{3/2}^{-4})(f_{7/2}^{2}p_{3/2}^{1})$	20.84	1.54	7.07	3.75
[11,6,3;2,0,1,0]	$(d_{5/2}^{-1}d_{3/2}^{-2}s_{1/2}^{-1})(f_{7/2}^{2}p_{3/2}^{1})$	0.82	1.32	0.51	0.51
[10,6,4;2,0,1,0]	$(d_{5/2}^{-2}d_{3/2}^{-2})(f_{7/2}^{2}p_{3/2}^{1})$	2.05	0.21	a	a
[12,4,4;1,0,2,0]	$(d_{3/2}^{-4})(f_{7/2}^{1}p_{3/2}^{2})$	1.41	1.19	1.79	4.56
[12,6,2;1,0,2,0]	$(d_{3/2}^{-2}s_{1/2}^{-2})(f_{7/2}^{1}p_{3/2}^{2})$	0.85	1.09	0.10	0.27
[12,5,3;1,0,2,0]	$(d_{3/2}^{-3}s_{1/2}^{-1})(f_{7/2}^{1}p_{3/2}^{2})$	3.14	0.45	0.68	0.37
[12,4,4;0,0,3,0]	$(d_{3/2}^{-4})(p_{3/2}^{3})$	2.02	0.00	0.18	0.10
[12,4,4;2,0,0,1]	$(d_{3/2}^{-4})(f_{7/2}^{2}p_{1/2}^{1})$	1.42	0.12	0.38	0.44
[12,4,4;2,1,0,0]	$(d_{3/2}^{-4})(f_{7/2}^{2}f_{5/2}^{1})$	0.05	0.78	0.60	1.56
[12,4,4;1,2,0,0]	$(d_{3/2}^{-4})(f_{7/2}^{1}f_{5/2}^{2})$	0.15	1.06	0.71	2.27
[12,4,4;1,0,0,2]	$(d_{3/2}^{-4})(f_{7/2}^{1}p_{1/2}^{2})$	0.00	0.79	0.22	0.91
[12,4,4;1,1,1,0]	$(d_{3/2}^{-4})(f_{7/2}^{1}f_{5/2}^{1}p_{3/2}^{1})$	0.82	0.21	0.28	0.34
Sum		90.66	92.57	96.19	97.64
$p_{1/2}$ orbit		4.04	2.23	1.99	2.62
$f_{5/2}$ orbit		4.38	6.35	3.81	2.27
$n(d_{5/2}) < 12$		10.98	13.06	9.77	6.73

[a]Omitted by the truncation.

3). The WBMB prediction for the $7/2^-$ ^{39}S ground-state binding energy is 325 250 keV, 180 keV less bound than experiment. The calculated binding energy of ^{39}Cl is 331 647 keV, 360 keV more bound than experiment.

An illustration of the good predictive powers of the USD and WBMB shell-model interaction is shown in Fig. 1, where the calculated binding energies of sulfur isotopes are compared to experiment. We also show a similar comparison to experiment for a recent finite-range droplet model[20] which is representative of semiempirical mass formulae.

Since the calculations for the odd-parity states of ^{39}Cl were, of necessity, carried out in a highly truncated basis, meaningful absolute binding energies for these states were not obtained. As shown in Fig. 2 and discussed in Sec. IV, the $^{39}S(\beta^-)^{39}Cl$ results of Hill *et al.*[5] imply an odd-

TABLE III. Even-parity ($2fp$) ^{39}Cl and odd-parity ($3fp$) ^{39}Cl and ^{39}S spectra calculated with the WBMB interaction. The $2fp$ ^{39}Cl and $3fp$ ^{39}S spectrum were generated from the full $sdfp$ model space. The $3fp$ ^{39}Cl spectrum was generated from a truncated model space as discussed in the text. All states are shown up to $3/2_8^+$ (for $2fp$) and $5/2_8^-$ (for $3fp$); after that only yrast states are listed.

$^{39}Cl(2fp)$			$^{39}Cl(3fp)$			$^{39}S(3fp)$		
E_x (keV)	J^π	No.	E_x (keV)	J^π	No.	E_x (keV)	J^π	No.
0	$3/2^+$	1	0	$7/2^-$	1	0	$7/2^-$	1
871	$1/2^+$	1	151	$3/2^-$	1	49	$3/2^-$	1
1 451	$5/2^+$	1	292	$5/2^-$	1	202	$5/2^-$	1
1 841	$7/2^+$	1	312	$1/2^-$	1	763	$3/2^-$	2
2 097	$3/2^+$	2	332	$7/2^-$	2	1 698	$11/2^-$	1
2 196	$1/2^+$	2	474	$9/2^-$	1	1 729	$1/2^-$	1
2 348	$5/2^+$	2	558	$9/2^-$	2	1 992	$9/2^-$	1
2 617	$3/2^+$	3	576	$3/2^-$	2	2 244	$7/2^-$	2
2 617	$9/2^+$	1	580	$5/2^-$	2	2 294	$5/2^-$	2
2 730	$5/2^+$	3	649	$7/2^-$	3	2 333	$9/2^-$	2
2 927	$11/2^+$	1	658	$11/2^-$	1	2 372	$7/2^-$	3
3 239	$9/2^+$	2	803	$7/2^-$	4	2 400	$1/2^-$	2
3 270	$7/2^+$	2	825	$1/2^-$	2	2 586	$5/2^-$	3
3 601	$3/2^+$	4	901	$5/2^-$	3	2 700	$3/2^-$	3
3 691	$7/2^+$	3	1 097	$3/2^-$	3	2 826	$3/2^-$	4
3 798	$15/2^+$	1	1 170	$3/2^-$	4	2 971	$5/2^-$	4
3 820	$5/2^+$	4	1 214	$7/2^-$	5	2 995	$3/2^-$	5
3 878	$9/2^+$	3	1 297	$5/2^-$	4	3 095	$7/2^-$	4
3 902	$1/2^+$	3	1 326	$9/2^-$	3	3 159	$11/2^-$	2
3 970	$3/2^+$	5	1 352	$11/2^-$	2	3 298	$5/2^-$	5
4 050	$7/2^+$	4	1 403	$13/2^-$	1	3 308	$7/2^-$	5
4 162	$11/2^+$	2	1 495	$7/2^-$	6	3 361	$9/2^-$	3
4 167	$13/2^+$	1	1 534	$9/2^-$	4	3 399	$15/2^-$	1
4 193	$5/2^+$	5	1 554	$5/2^-$	5	3 473	$5/2^-$	6
4 275	$3/2^+$	6	1 618	$7/2^-$	7	3 487	$3/2^-$	6
4 321	$5/2^+$	6	1 622	$3/2^-$	5	3 516	$1/2^-$	3
4 336	$7/2^+$	5	1 691	$5/2^-$	6	3 568	$5/2^-$	7
4 423	$5/2^+$	7	1 753	$5/2^-$	7	3 648	$11/2^-$	3
4 462	$13/2^+$	2	1 799	$9/2^-$	5	3 658	$7/2^-$	6
4 518	$11/2^+$	3	1 817	$3/2^-$	6	3 715	$3/2^-$	7
4 660	$9/2^+$	4	1 902	$3/2^-$	7	3 724	$9/2^-$	4
4 677	$3/2^+$	7	1 912	$5/2^-$	8	3 798	$7/2^-$	7
4 734	$7/2^+$	6	2 559	$15/2^-$	1	3 878	$1/2^-$	4
4 824	$9/2^+$	5	3 358	$17/2^-$	1	3 952	$13/2^-$	1
4 903	$7/2^+$	7	4 064	$19/2^-$	1	3 988	$5/2^-$	8
4 939	$1/2^+$	4	5 184	$21/2^-$	1	6 174	$19/2^-$	1
4 949	$3/2^+$	8	6 982	$23/2^-$	1	6 640	$17/2^-$	1
6 856	$17/2^+$	1	11 182	$25/2^-$	1	9 740	$21/2^-$	1
11 192	$19/2^+$	1	11 390	$27/2^-$	1	10 948	$23/2^-$	1
11 675	$21/2^+$	1	16 397	$29/2^-$	1	14 356	$25/2^-$	1
18 125	$23/2^+$	1	19 691	$31/2^-$	1	18 012	$27/2^-$	1
						22 683	$29/2^-$	1

parity spectrum commencing 1697 keV above the ^{39}Cl ground state. To accommodate this, we need to lower our calculated odd-parity excitation energies by 2.4 MeV. From our previous experience with truncation within the *sdfp* model space, this seems reasonable for the truncation used.

B. Beta and gamma decays

1. First forbidden beta decay

Because of the uncertainty in the J^π of the ^{39}S ground state (see Table III), the first-forbidden β^- decay of ^{39}S to the odd-parity ^{39}Cl states was calculated for assumed ^{39}S levels with $J^\pi = 3/2^-$, $5/2^-$, and $7/2^-$. The experimental Q_{β^-} value was used and the excitation energies of the ^{39}Cl $3/2_1^+$, $1/2_1^+$, $5/2_1^+$, and $7/2_1^+$ states were assumed to have the experimental values indicated by the correspondence between theory and experiment displayed in Fig. 2. Decays to all energetically accessible higher-lying states were considered. The excitation energies for these higher-lying states were taken from the predictions of Table III. The calculation was carried out with the effective operators described in Ref. 21. Using the ^{39}S half-life of 11.5(5) s (Ref. 5), we obtain the results given in Table IV. The results are pretty much as expected. For ^{39}S spins of 3/2 and 5/2 the decays are dominated by the rank-zero contribution to $\Delta J=0$ transitions. This is largely due to the mesonic enhancement of the timelike component of the axial current and is fully discussed by Warburton *et al.*[21] For $\Delta J=0$ first-forbidden transitions there is a $\Delta j=0$, $\Delta\pi=-$ restriction on the single-particle transition. Thus, the $f_{7/2}$ orbit cannot contribute and the matrix elements are largely due to transitions of the type $\nu(f_{7/2}^2 p_{3/2}) \rightarrow \nu(f_{7/2}^2)\pi(d_{3/2})$. The small decay rate for $7/2^- \rightarrow 7/2^+$ and the relatively small value for $3/2^- \rightarrow 3/2_1^+$ (as compared to the energy-unfavored decays to $3/2_2^+$ and $3/2_3^+$) is mainly due to destructive interference between contributing components of the above-mentioned type rather than to the smallness of these components. The predicted unique first-forbidden $7/2^- \rightarrow 3/2_1^+$ decay is relatively strong with a beta moment of $B_1 = 0.68$ fm^2 as compared, for instance, to the relatively large experimental value for ^{37}S$(7/2^-) \rightarrow ^{37}Cl(3/2_1^+)$ of $B_1 = 1.32(14)$ fm^2 (Ref. 21). The weakness of the total first-forbidden branching is due to the rather low-energy release for such a neutron-rich decay and the availability of low-lying odd-parity states for which allowed decays are possible. No first-forbidden branches were identified as such by Hill *et al.*[5] However, for all three assumed ^{39}S spins, the predicted first-forbidden branches to the yrast states are small compared to the experimental limits[5] on their existence.

TABLE IV. First-forbidden beta decay of ^{39}S to states of ^{39}Cl. Branching ratios (BR) are given to various states and groups of states for assumed spin parities of $3/2^-$, $5/2^-$, and $7/2^-$ for the ^{39}S ground state. For a single state, the f value is defined (Ref. 21) as $(61.66/11.5)\times$BR (%).

State(s)	Branching ratio (%) $3/2^-$	$5/2^-$	$7/2^-$
$3/2_1^+$; g.s.	2.04[a]	0.42	0.84
$1/2_1^+$; 396 keV	0.27	0.18	
$5/2_1^+$; 1302 keV	0.06	1.73	0.10
$7/2_1^+$; 1745 keV	0.01	0.02	0.03
Sum $(1/2_1^+, 3/2_1^+, 5/2_1^+, 7/2_1^+)$	2.38	2.35	0.97
Total first forbidden	6.02	2.37	1.20

[a]And 2.82% and 0.69% to $3/2_2^+$ and $3/2_3^+$, respectively.

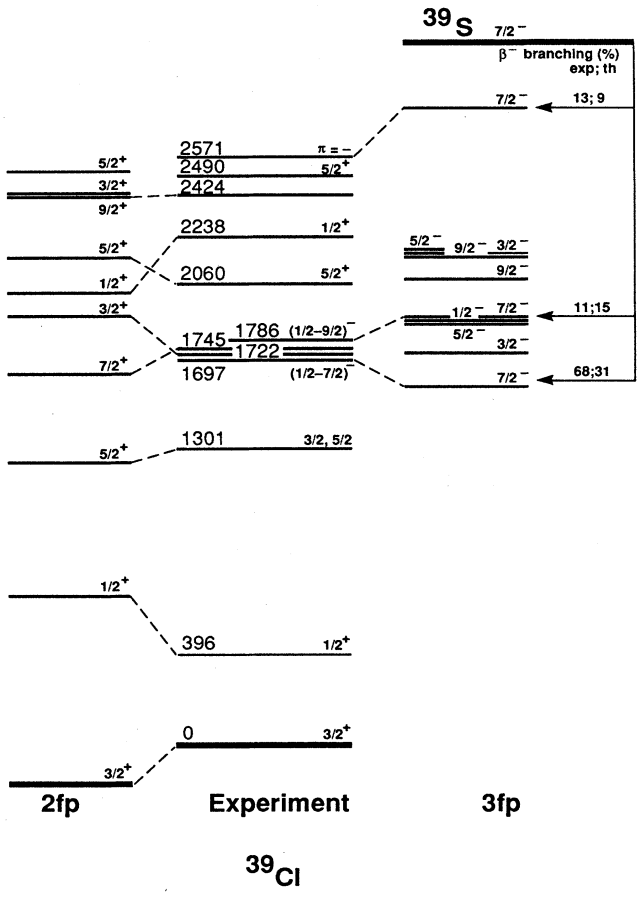

FIG. 2. Comparison of experimental and predicted ^{39}Cl energy spectra and β^- branching ratios. The experimental energy spectrum is discussed in the text. The $2fp$ even-parity spectrum is that of Table III with 192 keV subtracted from each energy. Except for the first two $7/2^-$ states (see the text), the odd-parity $3fp$ spectrum is that of Table III with 1576 keV added to each energy. The complete $3fp$ spectrum is shown up to 2200 keV after that only $7/2_5^-$ is shown. Experimental and predicted β^- branching ratios are compared under the assumption that the ^{39}S ground state is $7/2^-$.

2. Allowed beta decay

For the Gamow-Teller (GT) operator—and the similar $M1$ electromagnetic operator—Brown and Wilden-

TABLE V. Predictions for the allowed Gamow-Teller β^- decay of ^{39}S to ^{39}Cl. The $B(GT)$ values are calculated with the effective operator described in the text. $Log f_0 t$ is defined as $\log_{10}[6166/B(GT)]$. The Fermi integral f_0—and thus the β^- branching percentage, BR—is calculated with $Q_\beta = 6640$ keV and assuming the first two listed states for each J_i^π are at 1697 and 1786 keV (see Fig. 2) and the remainder have excitation energies obtained by adding 1576 keV to the ^{39}Cl $3fp$ excitation energies of Table III. The experimental $T_{1/2}$ is 11.5(5) s. The last line of the table gives the predicted $T_{1/2}$ and the percentage of the β^- decay proceeding to the lowest 15 states, i.e., those listed.

	$J_i^\pi = 3/2^-$				$J_i^\pi = 5/2^-$				$J_i^\pi = 7/2^-$		
J_k^π	$B(GT)$ ($\times 10^3$)	$\log f_0 t$	BR (%)	J_k^π	$B(GT)$ ($\times 10^3$)	$\log f_0 t$	BR (%)	J_k^π	$B(GT)$ ($\times 10^3$)	$\log f_0 t$	BR (%)
$3/2_1$	7.3	5.93	11.6	$7/2_1$	37.3	5.22	23.6	$7/2_1$	49.6	5.09	31.1
$5/2_1$	0.9	6.86	1.3	$7/2_2$	14.4	5.63	8.4	$7/2_2$	25.4	5.38	14.7
$1/2_1$	0.0	8.80	0.0	$3/2_1$	0.6	7.02	0.4	$5/2_1$	1.6	6.60	0.8
$5/2_2$	0.4	7.21	0.3	$5/2_1$	0.8	6.88	0.4	$9/2_1$	0.4	7.18	0.2
$3/2_2$	2.8	6.34	2.2	$3/2_2$	0.7	6.92	0.3	$9/2_2$	5.4	6.06	2.2
$5/2_3$	5.2	6.09	3.6	$5/2_2$	7.0	5.95	2.8	$5/2_2$	0.0	9.58	0.0
$1/2_2$	7.1	5.94	4.7	$7/2_3$	2.4	6.42	0.9	$7/2_3$	0.1	7.62	0.0
$3/2_3$	0.6	6.99	0.3	$7/2_4$	22.2	5.44	7.2	$7/2_4$	3.5	6.24	1.1
$3/2_4$	44.2	5.15	19.7	$5/2_3$	7.8	5.90	2.3	$5/2_3$	6.3	5.99	1.8
$5/2_4$	0.5	7.09	0.2	$3/2_3$	51.3	5.08	12.0	$7/2_5$	42.7	5.16	8.7
$3/2_5$	0.6	7.01	0.2	$3/2_4$	23.0	5.43	4.9	$5/2_4$	1.9	6.52	0.3
$5/2_5$	3.9	6.20	0.9	$7/2_5$	3.0	6.32	0.6	$9/2_3$	0.1	7.77	0.0
$3/2_6$	1.9	6.51	0.5	$5/2_4$	42.7	5.16	7.9	$7/2_6$	0.2	7.41	0.0
$5/2_6$	14.7	5.62	3.9	$7/2_6$	3.8	6.21	0.6	$9/2_4$	12.3	5.70	1.7
$5/2_7$	1.8	6.53	0.4	$5/2_5$	0.0	9.42	0.0	$5/2_5$	8.4	5.86	1.1
	$T_{1/2} = 10.6$ s, Σ (%) = 49.8				$T_{1/2} = 5.7$ s, Σ (%) = 72.3				$T_{1/2} = 5.6$ s, Σ(%) = 63.7		

thal[22,23] extracted effective operators for the *sd* shell from a least-squares fit to empirical GT and $M1$ matrix elements. We use their results for the *sd* shell. For the *fp* shell we use the fundamental results of Towner[24] modified to reproduce exactly the experimental $^{41}Sc(\beta^+)^{41}Ca$ GT matrix element and the ^{41}Ca and ^{41}Sc magnetic moments as explained in Ref. 3. This procedure gives $A = 41$ quenching factors of ~ 0.74 for the Gamow-Teller rate and ~ 0.92 and ~ 0.96 for the $M1$ isoscalar and isovector operators, respectively. It does allow some state dependence.

Gamow-Teller matrix elements were calculated for the decay of the ^{39}S ground state with spin J_i to all energetically accessible ^{39}Cl $J_i \pm 1$ states. The total needed was 20–50 for each final spin. Predictions for the Gamow-Teller beta strength, $B(GT)$, and $\log f_0 t$ values for the first 15 ^{39}Cl states of each possible spin are listed in Table V for $J_i^\pi = 3/2^-$, $5/2^-$, and $7/2^-$. These results will be compared to experiment in the next section.

3. Gamma decay

Electromagnetic $M1$ and $E2$ matrix elements were calculated for both the odd-parity, $3fp$ spectrum of ^{39}S and the even-parity, $2fp$ spectrum of ^{39}Cl. Matrix elements for all possible $\Delta J \leq 1$ $M1$ and $\Delta J \leq 2$ $E2$ transitions were calculated for the first three states of each spin. Results are available upon request to the authors. There is no experimental information available on γ decays in ^{39}S. For ^{39}Cl, the available information comes from the $^{37}Cl(t,p\gamma)^{39}Cl$ measurements of Warburton *et al.*[9] in which γ-ray branching ratios and level lifetimes were measured. We note that the angular correlations necessary to separate $M1$ and $E2$ contributions have not been performed nor have the ground-state magnetic dipole and electric quadrupole moments been measured. In Table VI we compare our predictions to experiment for the five lowest $2fp$ yrast levels assuming the correspondence between predicted and experimental levels indicated in Fig. 2. The two sets of $E2$ effective charges are those resulting from least-squares fits to *sd*-shell data with and without the constraint that the added incremental charge for neutrons and protons be equal.[26] The $E2$ matrix elements were calculated using an oscillator parameter of 1.950 fm. The columns labeled predicted values use the free-nucleon $M1$ operators (left side) and effective $M1$ operators (right side). The origin of the effective $M1$ operator was given in the preceding subsection. The results on the right are the preferred predictions for both $M1$ and $E2$ observables. The results on the left are also presented in order to give some feeling for the dependence of the results on the effective operators.

Our calculations of electromagnetic matrix elements in ^{39}Cl were confined to $M1$ and $E2$ decays between the $2fp$ levels. Decays involving the odd-parity levels were not considered for two reasons: (1) Our previous experience[3] has shown that the WBMB model space is inadequate for the calculation of $E1$ rates in the $A \sim 40$ region, and (2) the truncation of the $3fp$ model space is severe enough so that predictions of individual electromagnetic transition rates involving these states would be of limited value.

IV. COMPARISON TO EXPERIMENT

A. The ^{39}Cl level scheme

1. The energy spectrum

The predicted and experimental energy spectra are compared in Fig. 2. The experimental information is from Warburton *et al.*,[9] Hill *et al.*,[5] and Seeger.[8] The proton-pickup ^{40}Ar$(d,^3$He$)^{39}$Cl results of Seeger were obtained with polarized deuterons and give spin-parity assignments, as well as spectroscopic factors, to the levels at 0, 396, 2060, 2238, and 2490 keV. These results are of somewhat better quality but quite consistent with the earlier results of Wagner *et al.*[7] Unfortunately the energy resolution was not sufficient to resolve the quartet of levels at $\sim$1.7 MeV. The $(d,^3$He) results for this quartet are not in contradiction with the proposed identification of levels shown in Fig. 2. The 1301-, 2424-, and 2571-keV levels were not observed in the $(d,^3$He) studies. This is in agreement with expectations for the $5/2_1^+$ level (see Sec. IV A 2), and for $9/2^+$ and $\pi=-$ levels for which, in our model space, there is no pickup strength.

The ^{39}S$(\beta^-)^{39}$Cl results of Hill *et al.*[5] give the negative-parity assignments to the levels at 1697, 1786, and 2571 keV. These assignments are based on a presumption of odd parity for ^{39}S and $\log f_0 t$ values for the β decays to these levels of 5.06(22), 5.83(22), and 5.41(22) which we calculate using the branching ratios and β^- half-life given by Hill *et al.*[5] together with a Q_β value of 6640(53) keV.

The other data used in making the correspondence between the experimental and theoretical levels in Fig. 2 are the γ-decay data obtained in the ^{37}Cl$(t,p\gamma)^{39}$Cl reaction.[9] These data—which we shall review in Sec. IV A 3—suggest the $7/2_1^+$ assignment to the 1745-keV level.

In Fig. 2, the $2fp$ predicted spectrum has been shifted down by 192 keV which minimizes the rms difference for the eight levels for which a correspondence between ex-

TABLE VI. Comparison of experimental and predicted γ decays connecting the low-lying even-parity ($2fp$) states of ^{39}Cl. The $B(\lambda)$ are in Weisskopf units (W.u.), $\mu(M1)$ is in μ_N, $Q(E2)$ is in e b, mean lives are in ps, and branching ratios BR are in percent. The phase convention for the mixing ratio, $x(E2/M1)$, is that of Rose and Brink (Ref. 25). Powers of 10 are given in square brackets and uncertainties in parentheses. The experimental information is from Ref. 9. The $E2$ observables in the columns labeled predicted values are calculated with $e_p,e_n=1.35,0.35$ and 1.29,0.49, for the left and right columns, respectively. The $M1$ observables in the left column are calculated with the free-nucleon g factors while those in the right column use the effective g factors described in the text.

Initial state		Final state		E_γ	τ		Measured		
E_i (keV)	J^π	E_f (keV)	J^π	(keV)	(ps)	Quantity	value	Predicted values	
0	$3/2^+$	0	$3/2^+$			$\mu(M1)$		+0.3987	+0.5825
						$Q(E2)$		−9.617	−10.06
396	$1/2^+$	0	$3/2^+$	396	>2.0	$B(M1)$	<0.25	3.4[−2]	6.3[−2]
						$B(E2)$		4.22	4.87
						$x(E2/M1)$		−0.078	−0.061
						τ	>2	15.0	8.0
1302	$5/2^+$	396	$1/2^+$	906	>3.0	$B(E2)$	<4.6	1.57	1.82
						BR	6(2)	1.3	3.2
						τ (partial)	>38	109	94
		0	$3/2^+$	1302		$B(M1)$	<5.1[−3]	5.1[−3]	2.2[−3]
						$B(E2)$	<8.9	3.95	4.73
						$x(E2/M1)$		+0.633	+1.058
						BR	94(2)	99	97
						τ (partial)	>3.1	2.0	3.1
1745	$7/2^+$	1302	$5/2^+$	444	1.3(4)	$B(M1)$	10(3)[−2]	7.3[−2]	9.0[−2]
						$B(E2)$		7.41	7.29
						$x(E2/M1)$		+0.027	+0.024
						BR	37(4)	43	39
						τ (partial)	3.5(11)	5.0	4.0
		0	$3/2^+$	1745		$B(E2)$	3.1(9)	1.71	2.48
						BR	63(4)	57	61
						τ (partial)	2.1(6)	3.8	2.6
2424	$9/2^+$	1745	$7/2^+$	679	>1.8	$B(M1)$	<5.1[−3]	2.2[−4]	1.2[−6]
						$B(E2)$	<36.0	0.79	0.89
						$x(E2/M1)$		−10.4	+0.71
		1302	$5/2^+$	1123		$B(E2)$	<7.5	2.11	2.74

TABLE VII. WBMB predictions for the spectroscopic factor $\mathcal{S}_p^-$ for the proton pickup of ^{40}Ar to ^{39}Cl. The index k orders the ^{39}Cl states by excitation energy.

^{39}Cl state k	$1/2^+;0$	$J^\pi;l_p=$ $3/2^+;2$	$5/2^+;2$
1	1.64	2.20	0.05
2	0.36	0.11	0.26
3	0.02	0.08	0.31
4	0.00	0.03	0.06
5	0.00	0.01	0.00
$\sum$	2.02	2.44	0.68
$5/6\sum/\overline{p(j)}$	90%	83%	10%

periment and theory is made. The resulting rms deviation in excitation energies is 166 keV. As noted in Sec. III A, we calculate a ^{39}Cl ground state 360 keV more bound than experiment. For the eight levels in question, the average binding energy is in considerably better agreement with experiment—167 keV more bound than experiment.

2. *Spectroscopic strength in proton pickup from ^{40}Ar*

The WBMB predictions for the spectroscopic factor $\mathcal{S}_p^-$ for the proton pickup of ^{40}Ar to $1/2^+$, $3/2^+$, and $5/2^+$ states of ^{39}Cl are given in Table VII for the first five states ($k=1$–5) of each spin. The definition of $\mathcal{S}_p^-$ is such that

$$\sum_{\substack{\text{fixed } J_f \\ \text{all } k}} C^2\mathcal{S}_p^-(J_f,k)=\overline{p(j)}\ , \tag{6}$$

where $C^2=5/6$ for $^{40}Ar\rightarrow{}^{39}Cl+p$ and $\overline{p(j)}$ is the mean number of protons in the jth orbit in the ^{40}Ar ground state. The WBMB predictions are $\overline{p(d_{5/2})}=5.925$, $\overline{p(s_{1/2})}=1.874$, and $\overline{p(d_{3/2})}=2.202$. It is seen that most of the pickup strength is predicted to reside in the first few states for $J^\pi=1/2^+$ and $3/2^+$. Because the $d_{5/2}$ orbit is deeply bound, there is very little low-lying $d_{5/2}$ pickup strength; 68% of the total strength for $J^\pi=5/2^+$ is predicted to lie in the $k=11$–14 states between 5650 and 6320 MeV (see Table III). A detailed comparison to experiment is made in Table VIII for the low-lying states. The agreement is exceptionally good for the $1/2^+$ and $3/2^+$ states. For the $5/2^+$ states the overall agreement is quite poor, especially for higher-lying states which are not included in Tables VII and VIII. Seeger[8] found the $d_{5/2}$ pickup strength to be fragmented over considerably more $5/2^+$ states below 9-MeV excitation than are predicted in the WBMB $2fp$ model space. The disagreement suggests a redistribution of the spectroscopic strength due to $n\hbar\omega$ ($n=2,4,\ldots$) admixtures in the ^{40}Ar ground state and/or the $5/2^+$ ^{39}Cl levels. The same phenomenon was observed for the $5/2^+$ pickup strength in the $^{44}C(d,^3He)^{43}K$ reaction.[27] Note that the $1/2^+$ and $3/2^+$ pickup strength should not be nearly as sensitive to $n\hbar\omega$ admixtures since the $s_{1/2}$ and $d_{3/2}$ orbits lie much closer to the Fermi surface.

3. *^{39}Cl γ decay*

In Table VI we compare our predictions for the $1/2^+$, $3/2^+$, $5/2^+$, $7/2^+$, and $9/2^+$ yrast levels to the experimental information for the levels to which identify them in Fig. 2. It can be seen that the predictions are consistent with experiment and—in the few cases that quantitative comparison can be made—the agreement is quite good. For instance, for the 1745-keV level all known data are in agreement with the predictions (right side). The predictions for the other three even-parity levels identified in Fig. 2—those at 1722, 2060, and 2238 keV—are also consistent with experiment.

We have proposed a $7/2^-$ identification for the 1697-keV level. Warburton *et al.*[9] observed a partial Doppler shift of $F(\tau)=22(11)\%$ for the $1697\rightarrow0$ transition. This was interpreted to give a mean life of $\tau=1.1^{+1.4}_{-0.5}$ ps to the 1697-keV level. If the mean life were as short as 2.5 ps then the recommended upper limit (RUL) on $M2$ strengths[28] would rule out the $7/2^-$ possibility for the 1967-keV level. On reconsideration, this author (EKW) who was also involved in the $(t,p\gamma)$ study feels that the uncertainty on $F(\tau)$ was underestimated[29] and, in any case, $F(\tau)$ was within two standard deviations of zero. Thus we would recommend a limit $\tau>0.2$ ps for the 1697-keV level rather than the original $\tau=1.1^{+1.4}_{-0.5}$ ps.

TABLE VIII. Comparison of experimental and theoretical spectroscopic factors, $\mathcal{S}_p^-$, for $^{40}Ar(d,^3He)^{39}Cl$. The experimental values of $\mathcal{S}_p^-$ are from Seeger (Ref. 8) with uncertainties assigned as suggested by Endt (Ref. 28). Spin-parity assignments and level energies are from Warburton *et al.* (Ref. 9) and Seeger (Ref. 8).

J^π (Expt.)	J_k^π (assumed)	E_x (keV) (Expt.)	(WBMB)	l_p	$(2J+1)S_p^-$ (Expt.)	(WBMB)
$3/2^+$	$3/2_1^+$	0	0	2	2.6(6)	2.20
$1/2^+$	$1/2_1^+$	396	871	0	1.4(3)	1.36
(3/2,5/2)	$5/2_1^+$	1301	1451	2		0.05
$1/2-5/2^+$	$3/2_2^+$	1723	2097	2		0.11
$5/2^+$	$5/2_2^+$	2061	2348	2	0.8(2)	0.26
$1/2^+$	$1/2_2^+$	2238	2196	0	0.31(8)	0.36
$5/2^+$	$5/2_3^+$	2490	2730	2	0.24(6)	0.31

Warburton *et al.*[9] remarked that there was a significant probability for levels to be missed in the $(t,p\gamma)$ study. As seen in Fig. 2, the predicted density of odd-parity levels is considerably higher than can be accommodated by experimental candidates. Thus, the shell-model predictions reinforce the expectation that further experimental study would reveal additional ^{39}Cl levels in the 1.5–2.6 MeV region of excitation.

B. ^{39}S beta decay and the odd-parity levels of ^{39}Cl

We presented predictions for the Gamow-Teller decay of ^{39}S in Table V. These results assume an identification of the 1657- and 1786-keV levels with the first two model states which have appreciable beta strength, for otherwise we have severe disagreement with experiment. For a ^{39}S ground state of $5/2^-$ or $7/2^-$ these two model states are $7/2_1^-$ and $7/2_2^-$. The level ordering assumed for the remaining ^{39}Cl $3fp$ states is that of Table III and Fig. 2. The energy increment added to the ^{39}Cl $3fp$ spectrum of Table III to obtain the results of Fig. 2 is 1576 keV and this is the amount used for all but the first two levels in the calculation of f_0 values and β^- branching ratios. For a $3/2^-$ ^{39}S ground state we assume the 1697- and 1786-keV levels are the $3/2_1^-$ and $5/2_1^-$ states, respectively. We arbitrarily add the increment of 1576 keV to the remaining states in this case also.

Hill *et al.*[5] observed β^--delayed γ intensities which they interpreted to give β^- branches into the 1697-, 1786-, and 2541-keV levels of 68%, 11%, and 13%, respectively. We first note that our predictions for all three possible J_i^π is for considerable fragmentation of the β^- decay. Thus we predict that the intensities observed by Hill *et al.* contain considerable contributions from γ cascades from higher-lying levels. Bearing this in mind, we see that these relative values are in not too bad agreement with the model predictions for $J_i^\pi=5/2^-$ or $7/2^-$, but are in poor agreement for $J_i^\pi=3/2^-$. The best agreement is for $J_i^\pi=7/2^-$ with the 2571-keV level identified with $7/2_5^-$ as shown in Fig. 2. On the other hand, only $J_i^\pi=3/2^-$ gives a predicted $T_{1/2}$ in good agreement with experiment. It is clear that the model predictions of Table V are not of much help in fixing the spin-parity of the ^{39}S ground state. A spin-parity determination for ^{39}S can only be accomplished by further experimental work.

V. SUMMARY

Predictions have been given for binding energies, energy spectra, proton spectroscopic factors, and β^- and γ decay. The binding energy predictions for the ^{39}S and ^{39}Cl ground states are in good accord with experiment. The predicted even-parity energy spectrum of ^{39}Cl is in excellent agreement with the known properties. The root-mean-square deviation for the eight levels for which a correspondence is indicated in Fig. 2 is 166 keV.

The present even-parity ^{39}Cl level scheme is quite similar to that of Woods.[4] The differences are presumably due more to the differences in the interactions rather than in the model spaces.

First-forbidden beta decay was calculated with complete *sdfp* bases for the ^{39}Cl levels and the ^{39}S ground state. We consider the results quite reliable. We find a quite small contribution to the total β^- decay for all three assumed ^{39}S spins.

The allowed (Gamow-Teller) decay was calculated with a highly truncated *sdfp* basis for the ^{39}Cl odd-parity states. Thus the gross properties—such as the summed B(GT) strength and the total half-life—are expected to be considerably more reliable than the individual B(GT).

The comparison to experiment of Sec. IV has highlighted serious gaps in our knowledge of the spectroscopy of ^{39}Cl. More levels are expected below 2.6-MeV excitation and, for the known levels, information on spin-parities and electromagnetic matrix elements is severely lacking. It is startling that the magnetic and quadrupole moments of 56 min ^{39}Cl have not been measured. It is hoped that the predictions and comparison to experiment given here will help stimulate the further experimental work necessary for an understanding of these interesting neutron-rich nuclei.

ACKNOWLEDGMENTS

We thank B. A. Brown who suggested the truncation scheme used for the odd-parity states of ^{39}Cl and initiated the programming necessary to implement it. We also thank D. J. Millener for valuable discussions. This research was supported by the U.S. Department of Energy under Contract No. W-7405-Eng-48 with the University of California (Lawrence Livermore National Laboratory), Contract No. DE-AC02-76CH00016 with Brookhaven National Laboratory, and by an Alexander von Humboldt-Stiftung.

[1]E. K. Warburton and J. A. Becker, Phys. Rev. C **39**, 1535 (1989).
[2]E. K. Warburton, Phys. Rev. C **35**, 2278 (1987).
[3]E. K. Warburton, J. A. Becker, D. J. Millener, and B. A. Brown, Brookhaven National Laboratory Report 40890, 1987.
[4]C. L. Woods, Nucl. Phys. **A451**, 413 (1986).
[5]J. C. Hill, R. F. Petry, and K. H. Wang, Phys. Rev. C **21**, 384 (1980).
[6]G. Wang, E. K. Warburton, and D. E. Alburger, Phys. Rev. C **35**, 2272 (1987).
[7]G. J. Wagner, G. Th. Kaschl, G. Maire, U. Schmidt-Rohr, and P. Turek, Nucl. Phys. **A129**, 469 (1969).
[8]M. Seeger, Diplomarbeit, Max-Planck-Institut-für-Kernphysik, Heidelberg, 1987.
[9]E. K. Warburton, J. W. Olness, and G. A. P. Engelbertink, Phys. Rev. C **7**, 170 (1973).
[10]B. H. Wildenthal, Prog. Part. Nucl. Phys. **11**, 5 (1984).
[11]J. P. McGrory, Phys. Rev. C **8**, 693 (1973).
[12]D. J. Millener and D. Kurath, Nucl. Phys. **A255**, 315 (1975).
[13]B. A. Brown, A. Etchegoyen, W. D. M. Rae, and N. S. Godwin, OXBASH (unpublished)
[14]P. J. Brussaard and P. W. M. Glaudemans, *Shell-Model Applications in Nuclear Spectroscopy* (North-Holland, Amsterdam,

1977).
[15]D. H. Gloeckner and R. D. Lawson, Phys. Lett. **53B**, 313 (1974).
[16]D. J. Millener and E. K. Warburton (unpublished).
[17]P. V. Drumm, L. K. Fifield, R. A. Bark, M. A. C. Hotchis, and C. L. Woods, Nucl. Phys. **A469**, 530 (1989).
[18]It is tempting to speculate that the (^{13}C,^{14}O) reaction proceeds as a two-step (charge-exchange plus proton pickup) reaction which is selective of high spin and that the two ^{39}S groups observed correspond to the $7/2_1^-$ and $11/2_1^-$ levels. The latter is predicted at 1698 keV.
[19]A. H. Wapstra and G. Audi, Nucl. Phys. **A432**, 1 (1985).
[20]P. Möller, W. D. Meyers, W. J. Swiatecki, and J. Treiner, At. Data Nucl. Data Tables **39**, 225 (1988).
[21]E. K. Warburton, J. A. Becker, B. A. Brown, and D. J. Millener, Ann. Phys. (N.Y.) **187**, 471 (1988).
[22]B. A. Brown and B. H. Wildenthal, At. Data Nucl. Data Tables **33**, 347 (1985).
[23]B. A. Brown and B. H. Wildenthal, Nucl. Phys. **A474**, 2990 (1987).
[24]I. S. Towner, Phys. Rep. **155**, 264 (1987).
[25]H. J. Rose and D. M. Brink, Rev. Mod. Phys. **39**, 306 (1967).
[26]B. A. Brown, in Proceedings of the International Nuclear Physics Conference, Harrogate, United Kingdom, 1986.
[27]E. K. Warburton and D. E. Alburger, Phys. Rev. C **38**, 2822 (1988).
[28]P. M. Endt, At. Data Nucl. Data Tables **23**, 3 (1979).
[29]The relevant data are shown in Fig. 3 of Ref. 9. Specifically, we feel that the systematic error associated with the subtraction of the background underlying the 1697→0 transition was understimated.